Water electrolysis activated by Ru nanorod array electrodes

Seongyul Kim, Nikhil Koratkar, Tansel Karabacak, and Toh-Ming Lu

Citation: Applied Physics Letters **88**, 263106 (2006); doi: 10.1063/1.2218042
View online: http://dx.doi.org/10.1063/1.2218042
View Table of Contents: http://scitation.aip.org/content/aip/journal/apl/88/26?ver=pdfcov
Published by the AIP Publishing

Water electrolysis activated by Ru nanorod array electrodes

Seongyul Kim and Nikhil Koratkar[a)]
Department of Mechanical, Aerospace, and Nuclear Engineering, Rensselaer Polytechnic Institute, Troy, New York 12180

Tansel Karabacak and Toh-Ming Lu
Department of Physics, Applied Physics, and Astronomy, Rensselaer Polytechnic Institute, Troy, New York 12180

(Received 9 March 2006; accepted 12 May 2006; published online 27 June 2006)

Efficient hydrogen production is critical to fuel cell operation. One of the most convenient methods to produce hydrogen is via water electrolysis. However, overpotential losses at the cell electrodes results in poor efficiency. In this study we carried out water electrolysis experiments with ruthenium (Ru) nanorod arrays as the cathode. We show up to 25% reduction in overpotential and 20% reduction in energy consumption by use of the Ru nanorod cathode compared to the planar Ru cathode. We attribute the improvement to the increased active area of the nanostructured electrode which reduces the operating current density of the electrolyzer. © *2006 American Institute of Physics*. [DOI: 10.1063/1.2218042]

In recent years the attention focused on high-efficiency and low-polluting fuel cell vehicles has increased the demand for hydrogen as a vehicle fuel.[1,2] In addition to generating heat energy or electrical energy (as in fuel cells), hydrogen is also extensively used to make ammonia for fertilizer, in refineries to make reformulated gasolines, and in the chemical, food and metal industries. In the 21st century, hydrogen is poised to emerge as the primary energy carrier in a sustainable energy future.[2,3]

Hydrogen production techniques[1–6] can be divided into four categories: (1) biological, (2) chemical, (3) electrochemical such as water electrolysis, halide electrolysis, and H_2S electrolysis, and (4) thermal technologies. Among these water electrolysis is technologically very simple, does not create any corrosive by-products, and generates very high purity gases (hydrogen and oxygen) from water. Importantly water electrolysis is environmentally clean and no harmful waste products are released into the atmosphere (e.g., no carbon dioxide emissions). Additionally high purity oxygen (a byproduct of water electrolysis) is also extremely valuable, particularly for the semiconductor industry. Unlike other technologies, electrolysis does not require large, centralized plants and the cost of hydrogen production scales well from larger to smaller systems. Electrolysis units could therefore be widely distributed and scaled to meet hydrogen requirements of different users such as individual households, local fueling stations, and industrial facilities.

Electrolysis involves providing electrical energy[5,6] to dissociate water into the diatomic molecules of hydrogen and oxygen. Decomposition of water is a redox reaction—water is oxidized at the anode,

$$2H_2O \rightarrow O_2 + 4H^+ + 4e^-, \tag{1}$$

and reduced at the cathode,

$$4H_2O + 4e^- \rightarrow 2H_2 + 4OH^-. \tag{2}$$

The minimum necessary thermodynamic voltage ($V_{\text{cell}}^{\min}$) to start electrolysis is given[5] under standard conditions (pressure, temperature=const) as

$$V_{\text{cell}}^{\min} = \frac{-\Delta G^0}{nF}, \tag{3}$$

where $-\Delta G^0$ is the change in the Gibbs free energy under standard conditions, n is the number of electrons transferred, and F is Faraday's constant. In the case of an open cell, $V_{\text{cell}}^{\min}=1.23$ V, with $\Delta G^0=237.2$ kJ/mol (standard conditions, 1 bar, 25 °C). The above discussion pertains to an ideal case without any loss, but in practice, losses by reaction, diffusion, and resistance are inevitable resulting in a so-called overpotential. The operating voltage (V_{opt}) needed to drive the electrolysis cell at a current I is given[5] as,

$$V_{\text{opt}} = \frac{-\Delta G^0}{nF} + IR + \sum \eta, \tag{4}$$

where R is the total Ohmic series resistance in the cell including electrolyte, electrodes, and external series resistance; $\Sigma\eta$ is the sum of the overpotentials (activation overpotential at the anode, cathode, and the concentration overpotential due to mass transport of gaseous products away from the electrode surface). The energy (E) required to produce 1 mol of hydrogen can be expressed as

$$E = V_{\text{opt}} It, \tag{5}$$

where V_{opt} is the operating cell voltage, I is the driving current, and t is the time required to produce 1 mol of hydrogen.

In spite of the many advantages and attractive features of water electrolysis, it has yet to have a significant impact in terms of large scale hydrogen production. The principal reason for this is very high energy consumption, which makes these systems prohibitively expensive to operate. For example, the electricity consumption[1] for water electrolysis is about 4.5–5 kW h/m^3 in most industrial electrolyzers. This large energy consumption is related to the high overpotentials[7] [η in Eq. (4)] at both the anode and cathode, which are characteristic for gas evolution processes. These overpotentials are related to the interfacial phenomenon[3] in the three-phase zone where the gas bubble, electrolyte, and electrode surface contact each other. Our objective in this letter is to investigate whether nanostructured electrodes can enhance the efficiency of water electrolysis. We expect that

[a)]Author to whom correspondence should be addressed; electronic mail: koratn@rpi.edu

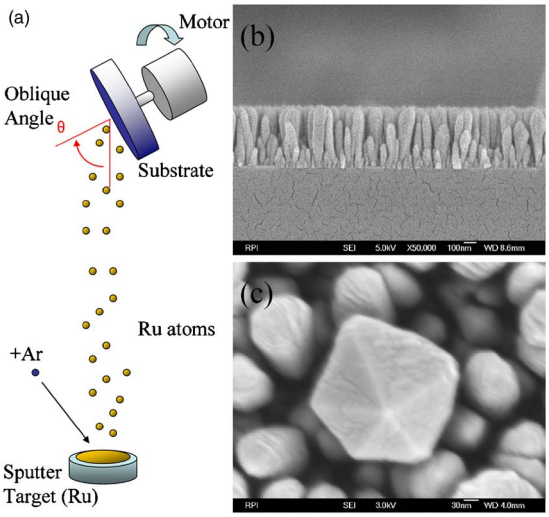

FIG. 1. (Color online) (a) Schematic of oblique angle deposition technique with substrate rotation used to fabricate the Ru nanorod arrays. (b) Scanning electron microscopy (SEM) image of side view of Ru nanorods. (c) SEM image of top view of Ru nanorods. The square base with pyramidal tip apex is clearly visible in the image.

the exposed surface area (or wetted area) for the nanostructured electrode will be greater than the planar electrode and this should lead to a significant reduction in the cell overpotential. While studies with nanostructured electrodes (featuring nanoparticle catalysts) have been reported for fuel cell electrodes[8,9] and for hydrolysis of chemical hydrides (e.g., lithium borohydride[10]), the activation of water electrolysis using Ru single-crystal nanorods has not yet been investigated in detail. The following sections of the letter will describe the oblique angle deposition technique[11–13] used to fabricate the Ru nanostructures, the water electrolysis experiments that were performed, and the conclusions from the study.

Ruthenium (Ru) was chosen for this study since it has good electrocatalytic properties and is well suited for water electrolysis. The Ru nanorods used in our experiments were grown on a Ni substrate using a 99.95% pure Ru cathode in a dc planar magnetron sputtering chamber with a base pressure of 4×10^{-7} Torr. The sputtering power used was 200 W at an argon pressure of 2.0 mTorr. The vapor flux arrived at an oblique incidence angle (θ=85°) from the substrate normal [Fig. 1(a) shows a schematic]. The limited adatom mobility combined with the shadowing effects due to the extremely oblique incidence with substrate rotating at 0.5 Hz results in the formation of isolated Ru nanorods[11–13] with pyramidal apex shaped tips. Scanning electron microscopy (SEM) images of the cross-section and top views of the Ru nanorods are shown in Figs. 1(b) and 1(c), respectively. The pyramidal shape tip apex with square base is clearly visible in these images. For metal deposition using oblique angle deposition, it is common that the competition between different crystal planes due to the minimization of surface energy would lead to a faceted surface such as the one shown in Fig. 1(c). Transmission electron microscopy and electron diffraction studies (not shown here) indicated that the Ru nanorods are actually single crystals.

Figure 2(a) shows a schematic for the nanostructured electrolyzer cell. Experiments were carried out by using an array of ruthenium (Ru) nanorods as the cathode. The anode is a Ni electrode and is polished to get mirror finish. The size

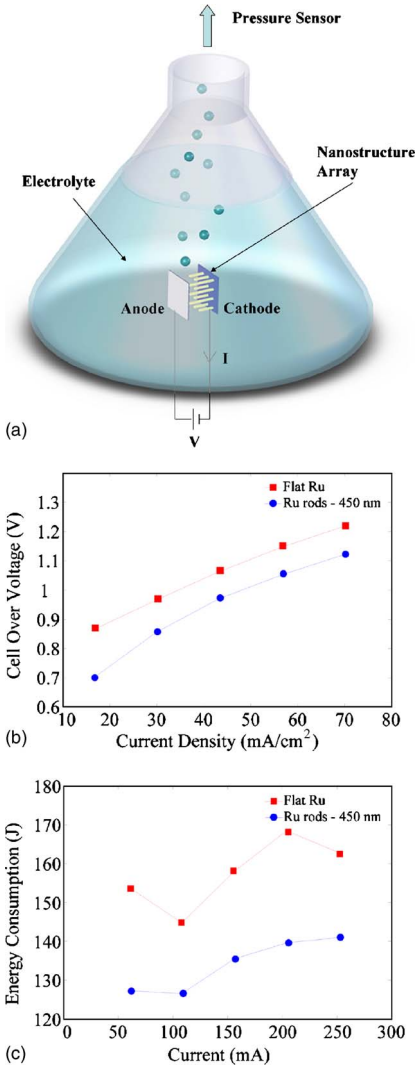

FIG. 2. (Color online) (a) Schematic of the nanostructured water electrolysis cell with Ru nanorod array as the cathode and planar Ni electrode as anode. The performance of the nanostructured electrolyzer was compared to a base line electrolyzer with planar Ru electrode as cathode and planar Ni electrode as anode. (b) Overpotential loss plotted as a function of the current density for the nanostructured electrolyzer and base line electrolyzer. The nanostructured electrolyzer shows significant (up to 25%) reduction in the overpotential. (c) Energy consumption of nanostructured electrolyzer and base line electrolyzer plotted as a function of current density. The nanostructured electrolyzer shows up to 20% reduction in energy consumption.

of the electrode plates used in the experiments was about 0.7×0.7 in.^{2} As shown in Fig. 2(a), the cell is housed within a flask containing KOH 30 wt % aqueous solution. To obtain constant gap, a glass spacer is inserted between the two electrodes. Each electrode is connected to a power supply and a constant (preset) current was applied to the electrodes while the potential difference between the electrodes was monitored. The current density was then computed by dividing the current by the exposed surface area of the electrode plate. The current density was varied in the 16–70 mA/cm^2 range in the experiments. A manometer was used to measure the pressure of the evolved hydrogen; the manometer pressure data were used to determine the amount of hydrogen produced.

The performance of the nanostructured electrolyzer (with Ru nanorods as the cathode and planar Ni anode) was then compared to a base line electrolyzer with planar Ru as the cathode and planar Ni as anode. Figure 2(b) shows the

cell overvoltage loss plotted as a function of current density. The literature[7,14] indicates that in the 0–100 mA/cm^2 current density range, the concentration and Ohmic overpotentials are small in comparison with the activation overpotential. Therefore the overpotentials shown in Fig. 2(b) are probably related to activation losses at the cell electrodes. For both the nanostructured electrolyzer and the base line electrolyzer, the overpotential loss increases with the current density; this is expected and similar trends are reported for industrial electrolyzer units. More importantly, the nanostructured electrolyzer shows very significant (up to 25%) reduction in the overpotential losses compared to the base line cell. In this test we used a Ru nanorod array (length ~450 nm) as cathode and a planar Ni sheet was employed as anode. This was done because in 0–100 mA/cm^2 range, the overpotential losses at the anode are expected to be relatively small[14] in comparison with the cathode. In addition to the overpotential, we also measured the electrical energy consumption [Eq. (5)]. The energy consumption of the nanostructured electrolyzer [see Fig. 2(c)] showed up to 20% reduction compared with the base line electrolyzer with planar electrodes.

We also studied the effect of length of the Ru nanorods on the electrolyzer performance. The results [Fig. 3(a)] indicate that there is no significant reduction in cell overvoltage as the nanorod length is increased from 130 to 450 nm. To investigate this further we measured the area of the pyramidal apex caps of the Ru nanorods using atomic force microscopy. The results indicate that irrespective of the length of the nanorods, the area of the pyramidal caps is about the same and corresponds to approximately twofold increase [Fig. 3(b)] compared to the planar flat electrode. This suggests that only the top caps of the Ru nanorods are electrochemically active because if this was the case then changing the rod length would not influence the active electrode area, which would explain the results shown in Fig. 3(a). Since the Ru nanorods are very densely packed it is very possible that only the top caps remain electrochemically active. To confirm this we scaled the current density for the nanorod samples by the increased apex cap area results shown in Fig. 3(b). The increased cap area lowers the operating current density, which causes a corresponding decrease in the overpotential. Figure 3(c) compares the overpotential after cap area scaling of the 130, 250, and 450 nm length Ru nanorod samples with that of the flat Ru electrode at an operating current density of ~16 mA/cm^2. The performance of all three nanorod samples is very close to that of the flat electrode, which confirms that the increased cap area of the nanorod cathode is primarily responsible for the improved performance of the nanostructured electrolyzer.

In this letter, we have shown that the overpotential loss and electric power consumption in a nanostructured water electrolyzer can be lowered by about 25% and 20%, respectively, compared to a planar electrolysis cell. We show that the observed performance improvement is related to the approximately twofold increase in effective wetted area offered by the Ru nanorod array compared to a planar Ru surface.

Funding support is acknowledged from the US National Science Foundation through NER and NIRT programs.

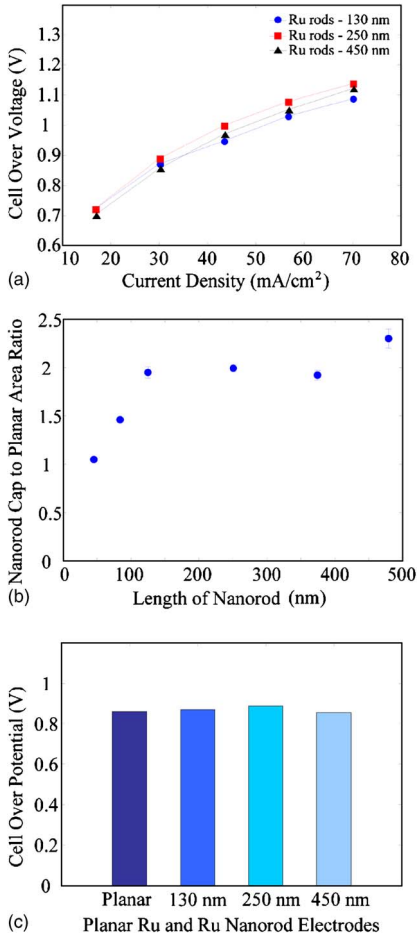

FIG. 3. (Color online) (a) Effect of Ru nanorod length on overpotential loss. The nanorod length has a relatively small influence on the overpotential loss. (b) Atomic force microscopy measurements for the nanorod apex cap area for different lengths of nanorods. The area of the apex caps is not significantly influenced by the nanorod length. (c) Overpotential loss for the different length nanorod samples after the current density is corrected to account for the increased nanorod apex cap area. The performance of the flat Ru electrode is also shown for comparison. The operating current density for all the samples after area correction is ~16 mA/cm^2.

[1]D. Stojic, M. Marceta, S. Sovilj, and S. Miljanic, J. Power Sources **118**, 315 (2003).
[2]E. Rasten, G. Hagen, and R. Tunold, Electrochim. Acta **48**, 3945 (2003).
[3]H. Matsushima, T. Nishida, Y. Konishi, Y. Fukunaka, Y. Ito, and K. Kuribayashi, Electrochim. Acta **48**, 4119 (2003).
[4]K. Onda, T. Kyakuno, K. Hattori, and K. Ito, J. Power Sources **132**, 64 (2004).
[5]C. Neagu, H. Jansen, H. Gardeniers, and M. Elwenspoek, Mechatronics **10**, 571 (2000).
[6]B. Campillo, P. Sebastian, S. Gamboa, J. Albarran, and L. Caballero, Mater. Sci. Eng., C **19**, 115 (2002).
[7]V. Ramani, H. R. Kunz, and J. M. Fenton, The Electrochemical Society Interface **13**, 3 (2004).
[8]A. Arico, P. Bruce, B. Scrosati, J.-M. Tarascon, and W. Van Schalkwijk, Nat. Mater. **4**, 366 (2005).
[9]K.-Y. Chan, J. Ding, J. Ren, S. Cheng, and K.-Y. Tsang, J. Mater. Chem. **14**, 505 (2004).
[10]Y. Kojima, K. Suzuki, and Y. Kawai, J. Power Sources **155**, 325 (2006).
[11]F. Tang, D.-L. Liu, D.-X. Ye, Y.-P. Zhao, T.-M. Lu, G.-C. Wang, and A. Vijayaraghavan, J. Appl. Phys. **93**, 4194 (2003).
[12]T. Karabacak, J. P. Singh, Y.-P. Zhao, G.-C. Wang, and T.-M. Lu, Phys. Rev. B **68**, 125408 (2003).
[13]J. P. Singh, G. R. Yang, T.-M. Lu, and G.-C. Wang, Appl. Phys. Lett. **81**, 4601 (2002).
[14]H. A. Liebhafsky and E. J. Cairns, *Fuel Cells and Fuel Batteries: A Guide to Their Research and Development* (Wiley, New York, 1969).